

Empty Cities: Image Inpainting for a Dynamic-Object-Invariant Space

Berta Bescos¹, José Neira¹, Roland Siegwart² and Cesar Cadena²

Abstract—In this paper we present an end-to-end deep learning framework to turn images that show dynamic content, such as vehicles or pedestrians, into realistic static frames. This objective encounters two main challenges: detecting the dynamic objects, and inpainting the static occluded background. The second challenge is approached with a conditional generative adversarial model that, taking as input the original dynamic image and the computed dynamic/static binary mask, is capable of generating the final static image. The former challenge is addressed by the use of a convolutional network that learns a multi-class semantic segmentation of the image. The objective of this network is producing an accurate segmentation and helping the previous generative model to output a realistic static image. These generated images can be used for applications such as virtual reality or vision-based robot localization purposes. To validate our approach, we show both qualitative and quantitative comparisons against other inpainting methods by removing the dynamic objects and hallucinating the static structure behind them. Furthermore, to demonstrate the potential of our results, we conduct pilot experiments showing the benefits of our proposal for visual place recognition. Code has been made available on <https://github.com/bertabescos/EmptyCities>.

I. INTRODUCTION

Dynamic objects degrade the performance of vision-based robotic pose-estimation or localization tasks. The standard approach to deal with dynamic objects consists on detecting them in the images, and further classifying them as not valid information for such purposes. However, we propose to instead modify these images so that the dynamic content is converted realistically into static. We consider that the combination of experience and context allows us to hallucinate, *i.e.*, inpaint, a geometrically and semantically consistent appearance of the static structure behind dynamic objects.

Turning images that contain dynamic objects into realistic static frames reveals several challenges:

- 1) Detecting such dynamic content in the image. By this, we mean to detect not only those objects that are known to move such as vehicles, people and animals, but also the shadows they might generate, since they also change the image appearance.
- 2) Inpainting the resulting space left by the detected dynamic content with plausible imagery. The resulting image would succeed in being realistic if the inpainted areas are both semantically and geometrically consistent with the static content of the image.

¹Berta Bescos and José Neira are with the Instituto de Investigación en Ingeniería de Aragón (I3A), Universidad de Zaragoza, Zaragoza 50018, Spain {bbescos, jneira}@unizar.es

²Roland Siegwart and Cesar Cadena are with the Autonomous Systems Lab (ASL), ETH Zürich, Zurich 8092, Switzerland {cesarc, rsiegwart}@ethz.ch



Fig. 1: Images at the same location with different dynamic content (top row) can be converted into the same static image, *i.e.*, a dynamic-object-invariant space (bottom row).

The former challenge can be addressed with geometrical approaches if a sequence of images is available. This procedure usually consists on studying the optical flow consistency along the images [1], [2]. In the case in which only one frame is available, deep learning is the approach that excels at this task by the use of Convolutional Neural Networks (CNNs) [3], [4]. These frameworks have to be trained with the previous knowledge of what classes are dynamic and which ones are not. Recent works show that it is possible to acquire this knowledge in a self-supervised manner [5], [6].

Regarding the second challenge, recent image inpainting approaches that do not use deep learning use image statistics of the remaining image to fill in the holes. The work of Telea [7] estimates the pixel value with the normalized weighted sum of all the known pixels in the neighbourhood. While this approach generally produces smooth results, it is limited by the available image statistics and has no concept of visual semantics. However, neural networks learn semantic priors and meaningful hidden representations in an end-to-end fashion, which have been used for recent image inpainting efforts [8], [9], [10], [11]. These networks employ convolutional filters on images, replacing the removed content with inpainted areas that usually have both geometrical and semantic consistency with the rest of the image.

Both challenges can also be seen as one single task: translating a dynamic image into a corresponding static image. In this direction, Isola *et al.* [12] propose a general-purpose solution for image-to-image translation.

In this paper we present an end-to-end deep learning framework to turn images that have dynamic content into realistic static frames. This can be used for many assorted applications such as cinematography, virtual reality and vision-based localization tasks, among others.

Just like Isola *et al.* [12] succeed in translating images

from day to night, aerial to map view, sketches to photos, semantic labels to street scene, *etc.*, our paper builds on their work to translate images from a space which is dynamic into a static one. The main difference between our objective and his is that, while they apply the same translation to the whole image, we want to keep the static areas of the image untouched, and translate the dynamic parts into static ones. We have adapted their framework to our specific task by introducing a new loss that, combined with the integration of the semantic segmentation network ERFNet [4] achieves the final objective of creating a dynamic objects invariant space. An example of our results can be seen in Fig. 1.

II. RELATED WORK

Previous works on SLAM in dynamic scenes have attempted to reconstruct the background occluded by dynamic objects in the images with information from previous frames [13], [14]. If only one frame is available, the occluded background can only be reconstructed by inpainting techniques.

Image Inpainting. Among the non-learning approaches to image inpainting, propagating appearance information from neighboring pixels to the target region is the usual procedure [7]. Accordingly, these methods succeed in dealing with narrow holes, where color and texture vary smoothly, but fail when handling big holes, resulting in over-smoothing. Differently, patch-based methods [15] operate by iteratively searching for relevant patches from the image non-hole regions. These approaches are computationally expensive and therefore not fast enough for real-time applications. Moreover, they do not make semantically aware patch selections.

Deep learning based methods usually initialize the image holes with a constant value, *e.g.*, the mean pixel value of the training dataset. This image is further passed through a CNN. Context Encoders [11] were among the first ones to successfully use a standard pixel-wise reconstruction loss, as well as an adversarial loss for image inpainting tasks. Due to the resulting artifacts, Yang *et al.* [16] take the result from Context Encoders as input and then propagates the texture information from non-hole regions to fill the hole regions as post-processing. Song *et al.* [17] use a refinement network in which a blurry initial hole-filling result is used as the input, then iteratively replaced with patches from the closest non-hole regions in the feature space. Iizuka *et al.* [10] extend Content Encoders by defining both global and local discriminators, then apply Poisson blending as a post-processing. Following this work, Yu *et al.* [9] replaced the post-processing with a refinement network powered by the contextual attention layers. The recent work of Liu *et al.* [8] obtains amazing inpainting results by using partial convolutions, *i.e.*, the output pixel of every layer is only conditioned on previous synthesized values.

In contrast, Ulyanov *et al.* [18] found that there is no need for external dataset training. The generative network itself can rely on its structure to complete the corrupted image. However, this approach usually applies several iterations (~ 50000) to achieve good and detailed results.

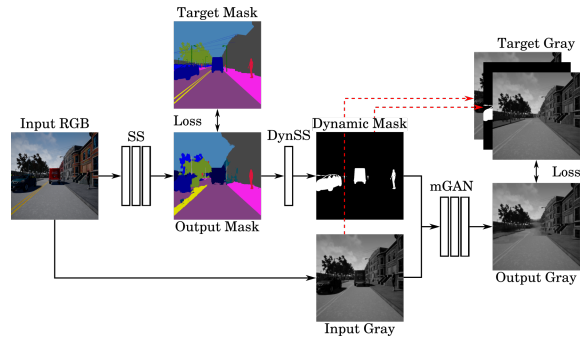


Fig. 2: Block diagram of our proposal. We first compute the segmentation of the RGB dynamic image, as well as its loss against the ground-truth mask. Both the mask and dynamic image are used to obtain the static image. Its loss is obtained and then back-propagated until the RGB dynamic image.

Our work does not perform pure inpainting but image-to-image translation with the help of a mask, coming from a semantic segmentation network. This means that we cannot initialize the “holes” with any placeholder values since we do not want to learn that pixels with this particular value have to be transformed. In our case, our input consists of the dynamic original image with the dynamic/static mask concatenated. Different from the other approaches, we perform this task in gray scale instead of in RGB. The motivation for this is that learning a mapping from $1D \rightarrow 1D$ instead of from $3D \rightarrow 3D$ is simpler and therefore leads to having less room for wrong reconstructions. In addition, many visual localization applications only need the images grayscale information. Still, as future work, we consider including a RGB version. Also, note that using the image-to-image translation approach allows us to slightly modify the image non-hole regions for better accommodation of the reconstructed areas.

III. SYSTEM DESCRIPTION

Fig. 2 shows an overview of our system during training time. First of all, we obtain the pixel-wise semantic segmentation of the RGB dynamic image (SS) and we compute its loss against the ground-truth mask. The segmentation of only the dynamic objects within this mask is obtained with the convolutional network DynSS. Once we have this mask, we convert the RGB dynamic image to gray scale and we compute the static image, also in gray scale, with the use of a U-Net, which has been trained in an adversarial way (mGAN). The loss of this generated image, in addition to the appearance L1 loss, is obtained and back-propagated until the RGB dynamic image, together with the previous computed mask loss. All the different stages, as well as the ground-truth generation, are described in subsections III-A to III-D.

A. Data Generation

We have explored our method using CARLA [19]. CARLA is an open-source simulator for autonomous driving research, that provides open digital assets (urban layouts, buildings, vehicles, pedestrians, *etc.*). The simulation platform supports flexible specification of sensor suites and environmental conditions. We have generated over 12000 image pairs consisting of a target image captured with

neither vehicles nor pedestrians, and a corresponding input image captured at the same pose with the same illumination conditions, but with cars, tracks and people moving around. These images have been recorded using a front and a rear RGB camera mounted on a car. Their ground-truth semantic segmentation has also been captured. CARLA offers two different towns that we have used for training and testing, respectively. Our dataset, together with more information about our framework, is available on <https://bertabescos.github.io/EmptyCities/>.

At present, we are limited to training on synthetic datasets since, to our knowledge, no real-world dataset exists that provides RGB images captured under same illumination conditions at identical poses over long trajectories, with and without dynamic objects. Recording a dataset ourselves would require huge amounts of both time and resources.

B. Dynamic-to-Static Translation

A Generative Adversarial Network (GAN) is a generative model that learns a mapping from a random noise vector z to an output image y , $G: z \rightarrow y$ [20]. In contrast, a conditional GAN (cGAN) learns a mapping from observed image x and optional random noise vector z , to y , $G: \{x, z\} \rightarrow y$ [21], or $G: x \rightarrow y$ [12]. The generator G is trained to produce outputs indistinguishable from “real” images by an adversarially trained discriminator, D , which is trained to do as well as possible at detecting the generator’s “fakes”.

The objective of a cGAN can be expressed as

$$\mathcal{L}_{cGAN}(G, D) = \mathbb{E}_{x,y}[\log D(x, y)] + \mathbb{E}_x[\log(1 - D(x, G(x)))], \quad (1)$$

where G tries to minimize this objective against an adversarial D that tries to maximize it. Previous approaches have found it beneficial to mix the GAN objective with a more traditional loss, such as L1 or L2 distance [11]. The discriminator’s job remains unchanged, but the generator is tasked not only with fooling the discriminator, but also with being near the ground-truth in a L1 sense, as expressed in

$$G^* = \arg \min_G \max_D \mathcal{L}_{cGAN}(G, D) + \lambda_1 \cdot \mathcal{L}_{L1}(G), \quad (2)$$

where $\mathcal{L}_{L1}(G) = \mathbb{E}_{x,y}[||y - G(x)||_1]$. The recent work of Isola *et al.* [12] shows that cGANs are suitable for image-to-image translation tasks, where the output image is conditioned on its corresponding input image, *i.e.*, it translates an image from one space into another (semantic labels to RGB appearance, RGB appearance to drawings, day to night, *etc.*). The main difference between our objective and his is that, while they apply the same mapping to the whole image, we want to keep untouched the static areas of the input image, and we want to translate the dynamic parts into static ones. This problem could also be seen as an inpainting problem. However, our method differs in that, in addition to changing the content of the image non-hole regions, it might also change the unmasked areas for a more

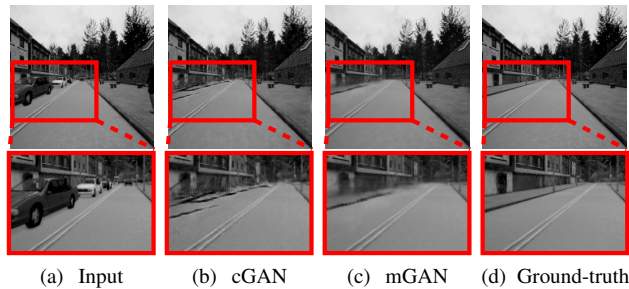


Fig. 3: Qualitative results of the improvements achieved by conditioning the discriminator on both input and mask (c), instead of only on the input (a), as conditional GANs do (b).

realistic output (for example, dynamic objects shadows could also be removed even if they are not masked).

It is well known that L2 and L1 losses produce blurry results on image generation problems, *i.e.*, they are capable of capturing the low frequencies but fail to encourage high frequency crispness. This motivates restricting the GAN discriminator to only model high frequency structures. Isola *et al.* [12] have adopted a discriminator architecture that penalizes structure at the scale of patches. That is, this discriminator tries to classify whether each $N \times N$ patch in an image is real or fake. All responses are finally averaged to provide the final output of the discriminator D .

For our objective, we adopt a variant of the cGAN that we call mGAN. mGANs learn a mapping from observed image x and binary mask m , to y , $G: \{x, m\} \rightarrow y$. When applying this to our case, we see that the dynamic objects in the image have been inpainted with high frequency texture but there are many artifacts (see Fig. 3b). One of the reasons is that, by applying the discriminator to the whole image, the fact that we are averaging its $N \times N$ responses reduces the influence of the few patches that look unrealistic on the final output, if all the other patches look realistic to the discriminator. As a solution to this problem, we propose to change the discriminator loss so that there is more emphasis on the main areas that have to be inpainted, according to

$$\mathcal{L}_{mGAN}(G, D) = \mathbb{E}_{x,y}[\log D_m(x, m, y)] + \mathbb{E}_x[\log(1 - D_m(x, m, G(x, m)))], \quad (3)$$

where $D_m(x, m, y) = D(x, y) \otimes (1 + m \cdot (\gamma - 1))$. The operator \otimes means the element-wise matrix product, and the parameter γ is a scalar that has been set to 2, as a good trade-off between the emphasis given to the masked compared to the unmasked areas. Fig. 3b shows our output if the discriminator is conditioned only on the input, in contrast with the discriminator conditioned on both the input and the mask (Fig. 3c). The last one shows more realistic results. This training procedure is diagrammed in Fig. 4.

C. Semantic Segmentation

Semantic Segmentation (SS) is a challenging task that addresses most of the perception needs of intelligent vehicles in a unified way. Deep neural networks excel at this task, as

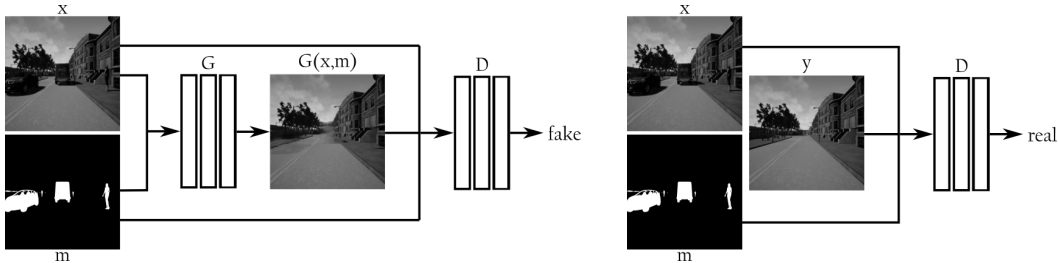


Fig. 4: The discriminator D has to learn to differ between the real images (y) and the images generated by the generator ($G(x, m)$). D is conditioned on the input mask m and the input image x .

they can be trained end-to-end to accurately classify multiple object categories in an image at pixel level. However, very few architectures have a good trade-off between high quality and computational resources. The recent work of Romera *et al.* [4] runs in real time while providing accurate semantic segmentation. The core of their architecture (ERFNet) uses residual connections and factorized convolutions to remain efficient while retaining remarkable accuracy.

Romera *et al.* [4] have made public some of their trained models [22]. We use for our approach the ERFNet model with encoder and decoder both trained from scratch on Cityscapes train set [23]. We have fine tuned their model to adjust it to our inpainting approach by back-propagating the loss of the mask $\mathcal{L}_{CE}(SS)$, calculated with the cross entropy criterion using the class weights they suggest, w , and the adversarial loss of our final inpainted model $\mathcal{L}_{mGAN}(G, D)$. The SS network’s job can be therefore expressed as:

$$SS^* = \arg \min_{SS} \max_D \mathcal{L}_{mGAN}(G, D) + \lambda_2 \cdot \mathcal{L}_{CE}(SS), \quad (4)$$

where $\mathcal{L}_{CE}(SS) = w[class] \cdot (\log(\sum_j \exp(y_{SS}[j])) - y_{SS}[class])$. Its objective is to produce an accurate semantic segmentation y_{SS} , but also to fool the discriminator D .

D. Dynamic Objects Semantic Segmentation

Once the semantic segmentation of the RGB image is done, we can select those classes known to be dynamic (vehicles and pedestrians). This has been done by applying a *SoftMax* layer, followed by a convolutional layer with a kernel of $n \times 1 \times 1$, where n is the number of classes, and with the weights of those dynamic and static channels set to w_{dyn} and w_{stat} respectively. w_{dyn} and w_{stat} are calculated following $w_{dyn} = \frac{n-n_{dyn}}{n}$ and $w_{stat} = -\frac{n_{dyn}}{n}$, where n_{dyn} stands for the number of dynamic existing classes.

The consequent output passes through a *Tanh* layer to obtain the wanted dynamic/static mask. Note that the defined weights w_{dyn} and w_{stat} are not changed during training time.

IV. EXPERIMENTAL RESULTS

A. Main Contributions

In this subsection we report the numerical improvements that have been achieved by using, for our particular case, gray-scale images instead of RGB images. We also show how the error drops down when using a generator G that learns a mapping from observed image x and binary mask

m to y , $G: \{x, m\} \rightarrow y$, instead of a mapping from image x to y , $G: x \rightarrow y$. Furthermore, we report how conditioning the discriminator on both the input and the binary mask $D(x, m, y)$, instead of on only the input $D(x, y)$, helps getting better results. These results are shown in Table I.

Experiment	$G(x)_{RGB}$ $D(x, y)_{RGB}$	$G(x)$ $D(x, y)$	$G(x, m)$ $D(x, y)$	$G(x, m)$ $D(x, m, y)$
$\mathcal{L}_1(\%)$	2.27	1.87	1.21	0.97
$\mathcal{L}_{1mask}(\%)$	9.87	9.17	6.69	6.00
$\mathcal{L}_{1no.mask}(\%)$	2.02	1.61	1.00	0.78

TABLE I: Quantitative evaluations of the achievements carried out by our contributions in the inpainting task. This evaluation has been made on the test synthetic images.

As mentioned in the work of Yu *et al.* [9], there is no good numerical metric to evaluate image inpainting results due to the existence of many possible solutions. Nevertheless, we follow previous image inpainting works and report \mathcal{L}_1 error. Using RGB images usually leads to obtaining inpainting efforts on areas that are colorful such as cars, but also road signals and traffic lights, that we certainly want to keep untouched. We see that the main improvement carried out by working in gray scale is in the unmasked areas $\mathcal{L}_{1no.mask}$. By using the mask to train both the generator G and the discriminator D , we obtain a more accurate static-to-dynamic translation in the masked areas \mathcal{L}_{1mask} , as well as in the unmasked ones. Results reported from now on within the text are obtained with the generator $G(x, m)$ and the discriminator $D(x, m, y)$, *i.e.*, with mGANs.

B. Inpainting Comparisons

We compare qualitatively and quantitatively our “inpainting” method with three other approaches:

- **Geo**: a state-of-the-art non-learning based approach [7].
- **Lea1, Lea2**: two deep learning based methods [9], [10].

Since both **Lea1** and **Lea2** are methods conceived for general inpainting purposes, we directly use their released models [9], [10] trained on the Places2 dataset [24]. We provide them with the same mask than to our method to generate the holes in the images. We evaluate qualitatively on the 3000 images from our synthetic test dataset, and on the 500 validation images from the Cityscapes dataset [23]. We can see in Figs. 5 and 6 the qualitative comparisons on both datasets respectively. Note that results generated with both

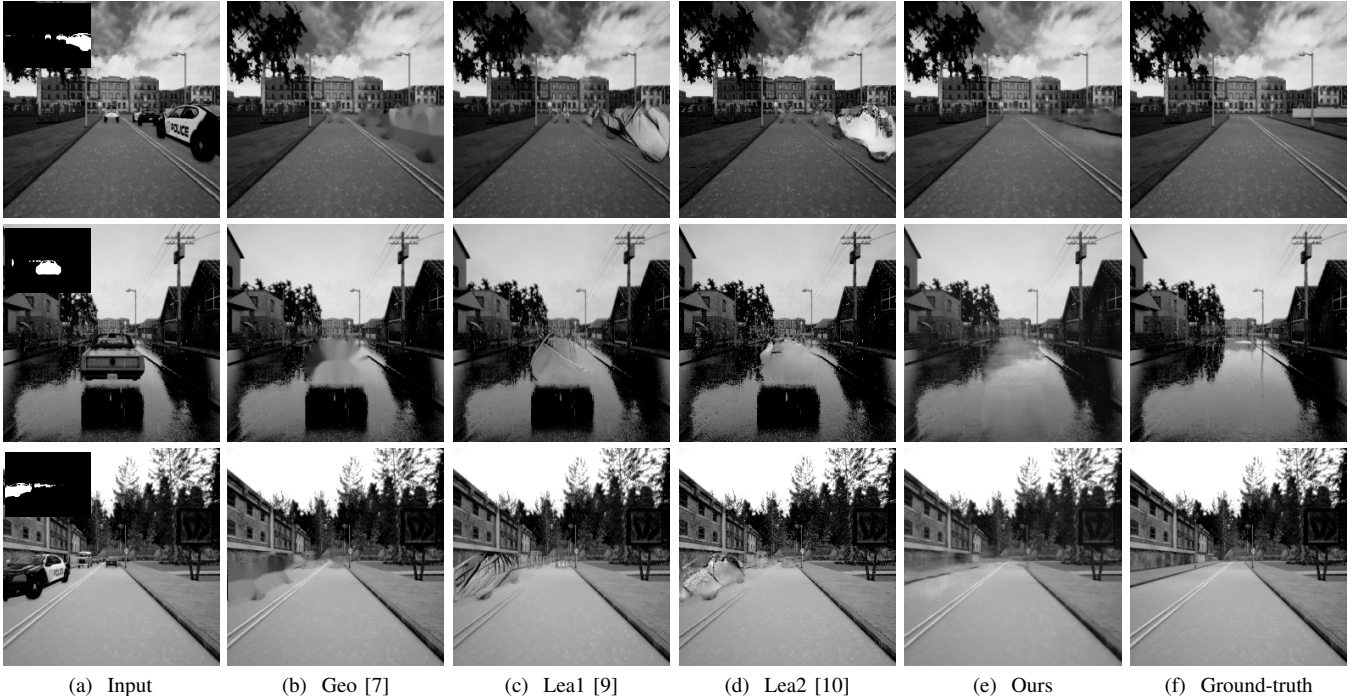


Fig. 5: Qualitative comparison of our method (e) against other inpainting techniques (b), (c), (d) on our synthetic dataset.

Lea1 and **Lea2** have been generated with the color images and then converted to gray scale for visual comparison. In the case of **Lea2**, the images have been first resized to a 256×256 resolution, since all their models have been trained with these image sizes. Albeit, Iizuka *et al.* [10] claim that their method works with images of any size, and therefore the images have been processed at their original resolution. Visually, we see that our method obtains a more realistic output. Also, it is the only one capable of removing the shadows generated by the dynamic objects even though they are not included in the dynamic/static mask (Fig. 5 row 2). The utilized masks are included in the images in Fig. 5a.

Table II shows the quantitative comparison of our method against **Geo**, **Lea1** and **Lea2** on our CARLA dataset. It is not possible to quantitatively measure the performance of the different methods on the Cityscapes dataset, since ground-truth does not exist. By following these results, we can claim that our method outperforms both qualitatively and quantitatively the other approaches in such task.

Experiment	Geo [7]	Lea1 [9]	Lea2 [10]	Ours
$\mathcal{L}_{1mask}(\%)$	6.66	10.45	10.49	6.00

TABLE II: Quantitative results of our method against other inpainting approaches in our CARLA dataset.

C. Transfer to Real Data

There is mounting evidence that models trained on synthetic data can nevertheless be useful for real world vision tasks [25], [26], [27], [28]. Accordingly, we provide a preliminary study of synthetic-to-real transfer learning using data from the Cityscapes dataset [23], which offers a variety of real-world environments similar to the synthetic ones.

When testing our method on real data, we see qualitatively that results are not as good as with the CARLA images (Fig. 6e). This happens because such data has different statistics than the real one, and therefore cannot be easily used. The combination of real and synthetic data is possible during training despite the lack of ground-truth static real images. In the case of the real images, the network only learns the texture and the style of the real world by encoding its information and decoding back the original image. The synthetic data is substantially more plentiful and has information about the inpainting process. The rendering, however, is far from realistic. Thus, the chosen representation attempts to bridge the reality gap encountered when using simulated data, and to remove the need for domain adaptation.

Fig. 6f shows how adding real images in the training process leads the testing in real data to give slightly better results. Also, to further reduce overfitting to the synthetic data, we perform extensive data augmentation by adding Gaussian blur, Gaussian noise, as well as brightness, contrast and saturation variation. Still, the results are not as accurate/realistic as the ones obtained with the CARLA images.

D. Visual Localization Experiments

We believe that the images generated by our framework have a potential use for visual localization tasks. As a proof of concept, we conduct three additional experiments.

First, we generated a CARLA dataset consisting of 20 different locations with 6 images taken per location. These 6 images show a different dynamic objects setup (Fig. 1). Then the global descriptors (from an off-the-shelf CNN [29]) computed from the different versions of the same location were compared. The euclidean distance between the descriptors

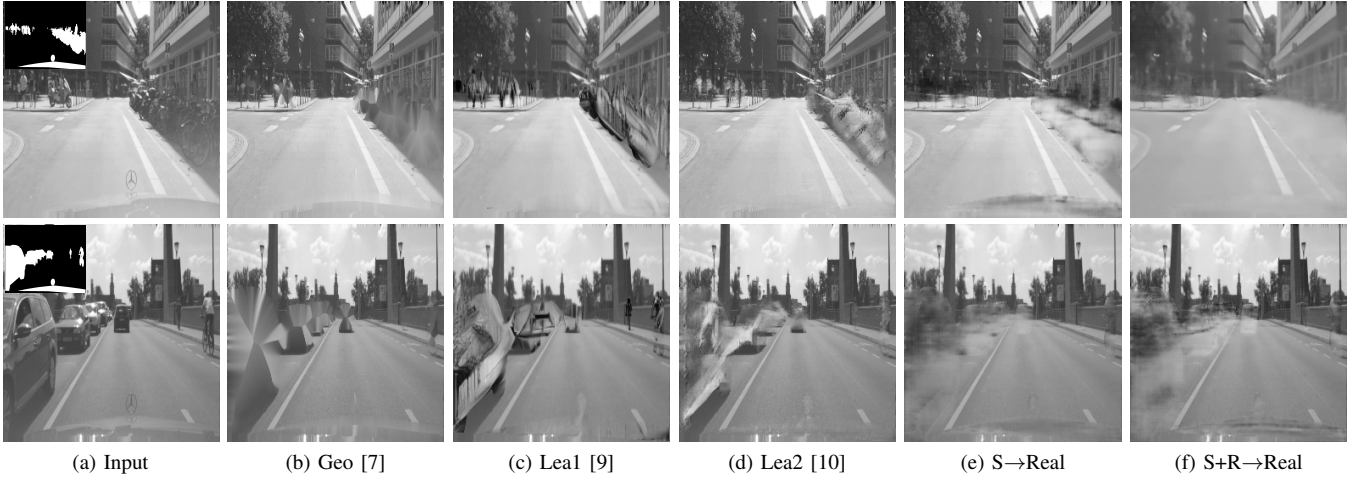


Fig. 6: Qualitative comparison of our method (e), (f) against other image inpainting approaches (b), (c), (d) on the Cityscapes dataset [23]. (e) shows our results when the training images are all synthetic. Albeit, (f) shows our results when real images from the Cityscapes dataset have been incorporated to our training set together with the synthetic CARLA images.



Fig. 7: (a) and (b) show the same location at different times with different viewpoints, weather conditions and dynamic objects setups [30]. The place recognition work by Olid *et al.* [29] fails to match them as the same place. However, it succeeds in matching them when our framework is previously employed –(c) and (d)–.

of the scenes with dynamic objects was always greater than that of the images after dynamic removal and inpainting. A 32% average reduction in the distance was observed.

In the second experiment, we generated 6 CARLA images at 6 different locations with a very similar vehicle setup. With the same global descriptor used in the previous experiment, we compared the distances between all possible image pair combinations. Then, we obtained the inpainted images with our framework, and computed the same distances. We repeated this experiment 4 times varying the vehicle setup used and saw that the mean distance of the inpainted sets was higher than that of the original images by 65%.

The third experiment was conducted with real world images from the SVS dataset [30]. We performed place recognition [29] with both the original images, and the ones processed by our framework. In the first case, this task was successful in 58% of the cases, whereas with our images the success rate was of 67%. Fig. 7 shows a case in which our framework makes place recognition successful.

From these results, we see that our framework brings closer images from the same place with different dynamic objects while pulling apart images from different places but with similar dynamic objects. We are confident that localization and mapping systems could benefit from these advances. Also, we expect similar methods to show comparable improvements by incorporating our proposal. Furthermore, a

strong benefit of our approach is that such methods would require no modification to work with our processed images.

E. Timing Analysis

Reporting our framework efficiency is crucial to judge its suitability for robotic tasks. The end-to-end pipeline runs at 50 fps on a nVidia GeForce GTX 1070 8GB with images of a 256×256 resolution. Out of the 20 ms it takes to process one frame, 18 ms are invested into obtaining its SS, and 2 ms are used for the inpainting task. Other than to deal with dynamic objects, the SS may be needed for many other tasks involved in automatic navigation. In such cases, our framework would only add 2 extra ms per frame. Based on our analysis, we consider that the inpainting task is not the bottleneck, even though higher resolution images may be needed.

V. CONCLUSION

We have presented an open-source end-to-end deep learning framework that takes as input a RGB image from a city environment containing dynamic objects such as cars, and converts it into a gray realistic image with only static content. For this objective, we develop mGANs, an adaptation of generative adversarial networks for inpainting problems.

The provided comparison against other state-of-the-art inpainting methods shows that our approach performs better. Also, our approach has a feature that makes it different from other inpainting methods: areas of the non-hole image can be changed for the objective of a more realistic output.

The visual localization experiments show that localization and mapping systems can benefit from our advances with the great advantage of not requiring any further modification.

Future extensions of this work might include, among others, converting the resulting static images from gray scale to color by following, for example, the approach of Li *et al.* [31]. Also, we consider exploiting multi-resolution images models, as well as making more research efforts into its transferability to other domains, *i.e.*, real world images.

REFERENCES

- [1] Y. Wang and S. Huang, "Motion segmentation based robust RGB-D SLAM," in *Intelligent Control and Automation (WCICA), 2014 11th World Congress on*, pp. 3122–3127, IEEE, 2014.
- [2] P. F. Alcantarilla, J. J. Yebes, J. Almazán, and L. M. Bergasa, "On combining visual SLAM and dense scene flow to increase the robustness of localization and mapping in dynamic environments," in *Robotics and Automation (ICRA), 2012 IEEE International Conference on*, pp. 1290–1297, IEEE, 2012.
- [3] K. He, G. Gkioxari, P. Dollár, and R. Girshick, "Mask R-CNN," in *Computer Vision (ICCV), 2017 IEEE International Conference on*, pp. 2980–2988, IEEE, 2017.
- [4] E. Romera, J. M. Alvarez, L. M. Bergasa, and R. Arroyo, "ERFNet: Efficient Residual Factorized ConvNet for Real-Time Semantic Segmentation," *IEEE Transactions on Intelligent Transportation Systems*, vol. 19, no. 1, pp. 263–272, 2018.
- [5] D. Barnes, W. Maddern, G. Pascoe, and I. Posner, "Driven to distraction: Self-supervised distractor learning for robust monocular visual odometry in urban environments," *arXiv preprint arXiv:1711.06623*, 2017.
- [6] G. Zhou, B. Bescos, M. Dymczyk, M. Pfeiffer, J. Neira, and R. Siegwart, "Dynamic objects segmentation for visual localization in urban environments," *arXiv preprint arXiv:1807.02996*, 2018.
- [7] A. Telea, "An image inpainting technique based on the fast marching method," *Journal of graphics tools*, vol. 9, no. 1, pp. 23–34, 2004.
- [8] G. Liu, F. A. Reda, K. J. Shih, T.-C. Wang, A. Tao, and B. Catanzaro, "Image inpainting for irregular holes using partial convolutions," *arXiv preprint arXiv:1804.07723*, 2018.
- [9] J. Yu, Z. Lin, J. Yang, X. Shen, X. Lu, and T. S. Huang, "Generative Image Inpainting with Contextual Attention," *arXiv preprint arXiv:1801.07892*, 2018.
- [10] S. Iizuka, E. Simo-Serra, and H. Ishikawa, "Globally and locally consistent image completion," *ACM Transactions on Graphics (TOG)*, vol. 36, no. 4, p. 107, 2017.
- [11] D. Pathak, P. Krahenbuhl, J. Donahue, T. Darrell, and A. A. Efros, "Context encoders: Feature learning by inpainting," in *Proceedings of the IEEE Conference on Computer Vision and Pattern Recognition*, pp. 2536–2544, 2016.
- [12] P. Isola, J.-Y. Zhu, T. Zhou, and A. A. Efros, "Image-to-image translation with conditional adversarial networks," *arXiv preprint*, 2017.
- [13] B. Bescos, J. M. Fácil, J. Civera, and J. Neira, "DynaSLAM: Tracking, Mapping and Inpainting in Dynamic Scenes," *arXiv preprint*, 2018.
- [14] R. Scona, M. Jaimez, Y. R. Petillot, M. Fallon, and D. Cremers, "StaticFusion: Background Reconstruction for Dense RGB-D SLAM in Dynamic Environments," in *Robotics and Automation (ICRA), 2018 IEEE International Conference on*, Institute of Electrical and Electronics Engineers, 2018.
- [15] A. A. Efros and W. T. Freeman, "Image quilting for texture synthesis and transfer," in *Proceedings of the 28th annual conference on Computer graphics and interactive techniques*, pp. 341–346, ACM, 2001.
- [16] C. Yang, X. Lu, Z. Lin, E. Shechtman, O. Wang, and H. Li, "High-resolution image inpainting using multi-scale neural patch synthesis," in *The IEEE Conference on Computer Vision and Pattern Recognition (CVPR)*, vol. 1, p. 3, 2017.
- [17] Y. Song, C. Yang, Z. Lin, H. Li, Q. Huang, and C.-C. J. Kuo, "Image inpainting using multi-scale feature image translation," *arXiv preprint arXiv:1711.08590*, 2017.
- [18] D. Ulyanov, A. Vedaldi, and V. Lempitsky, "Deep image prior," *arXiv preprint arXiv:1711.10925*, 2017.
- [19] A. Dosovitskiy, G. Ros, F. Codevilla, A. López, and V. Koltun, "Carla: An open urban driving simulator," *arXiv preprint arXiv:1711.03938*, 2017.
- [20] I. Goodfellow, J. Pouget-Abadie, M. Mirza, B. Xu, D. Warde-Farley, S. Ozair, A. Courville, and Y. Bengio, "Generative adversarial nets," in *Advances in neural information processing systems*, pp. 2672–2680, 2014.
- [21] J. Gauthier, "Conditional generative adversarial nets for convolutional face generation," *Class Project for Stanford CS231N: Convolutional Neural Networks for Visual Recognition, Winter semester*, vol. 2014, no. 5, p. 2, 2014.
- [22] E. Romera, J. M. Alvarez, L. M. Bergasa, and R. Arroyo, "ERFNet," <https://github.com/Eromera/erfnet>, 2017.
- [23] M. Cordts, M. Omran, S. Ramos, T. Rehfeld, M. Enzweiler, R. Benenson, U. Franke, S. Roth, and B. Schiele, "The cityscapes dataset for semantic urban scene understanding," in *Proceedings of the IEEE conference on computer vision and pattern recognition*, pp. 3213–3223, 2016.
- [24] B. Zhou, A. Lapedriza, A. Khosla, A. Oliva, and A. Torralba, "Places: A 10 million image database for scene recognition," *IEEE Transactions on Pattern Analysis and Machine Intelligence*, 2017.
- [25] A. Gaidon, Q. Wang, Y. Cabon, and E. Vig, "Virtual worlds as proxy for multi-object tracking analysis," *arXiv preprint arXiv:1605.06457*, 2016.
- [26] M. Peris, S. Martull, A. Maki, Y. Ohkawa, and K. Fukui, "Towards a simulation driven stereo vision system," in *Pattern Recognition (ICPR), 2012 21st International Conference on*, pp. 1038–1042, IEEE, 2012.
- [27] J. Skinner, S. Garg, N. Sünderhauf, P. Corke, B. Upcroft, and M. Milford, "High-fidelity simulation for evaluating robotic vision performance," in *Intelligent Robots and Systems (IROS), 2016 IEEE/RSJ International Conference on*, pp. 2737–2744, IEEE, 2016.
- [28] J. Tobin, R. Fong, A. Ray, J. Schneider, W. Zaremba, and P. Abbeel, "Domain randomization for transferring deep neural networks from simulation to the real world," in *Intelligent Robots and Systems (IROS), 2017 IEEE/RSJ International Conference on*, pp. 23–30, IEEE, 2017.
- [29] D. Olid, J. M. Fácil, and J. Civera, "Single-view place recognition under seasonal changes," *arXiv preprint arXiv:1808.06516*, 2018.
- [30] F. Werburg and J. Civera, "Street View Sequences: A dataset for lifelong place recognition with viewpoint and dynamic changes," *arXiv*, 2018.
- [31] Y. Li, M.-Y. Liu, X. Li, M.-H. Yang, and J. Kautz, "A closed-form solution to photorealistic image stylization," *arXiv preprint arXiv:1802.06474*, 2018.